PNAS RESEARCH ARTICLE | MICROBIOLOGY

A genome-wide CRISPR/Cas9 screen identifies a role for Rab5A and early endosomes in hepatitis E virus replication

Noémie Oechslin[a], Nathalie Da Silva[a], Maliki Ankavay[a], Darius Moradpour[a,1], and Jérôme Gouttenoire[a,1]

Edited by Charles Rice, Rockefeller University, New York, NY; received May 8, 2023; accepted November 17, 2023

Hepatitis E virus (HEV) is a major cause of acute hepatitis worldwide. As the other positive-strand RNA viruses, it is believed to replicate its genome in a membrane-associated replication complex. However, current understanding of the host factors required for productive HEV infection is limited and the site as well as the composition of the HEV replication complex are still poorly characterized. To identify host factors required for HEV RNA replication, we performed a genome-wide CRISPR/Cas9 screen in permissive human cell lines harboring subgenomic HEV replicons allowing for positive and negative selection. Among the validated candidates, Ras-related early endosomal protein Rab5A was selected for further characterization. siRNA-mediated silencing of Rab5A and its effectors APPL1 and EEA1, but not of the late and recycling endosome components Rab7A and Rab11A, respectively, significantly reduced HEV RNA replication. Furthermore, pharmacological inhibition of Rab5A and of dynamin-2, required for the formation of early endosomes, resulted in a dose-dependent decrease of HEV RNA replication. Colocalization studies revealed close proximity of Rab5A, the HEV ORF1 protein, corresponding to the viral replicase, as well as HEV positive- and negative-strand RNA. In conclusion, we successfully exploited CRISPR/Cas9 and selectable subgenomic replicons to identify host factors of a noncytolytic virus. This approach revealed a role for Rab5A and early endosomes in HEV RNA replication, likely by serving as a scaffold for the establishment of functional replication complexes. Our findings yield insights into the HEV life cycle and the virus–host interactions required for productive infection.

hepatitis E virus | Rab5A | early endosome | replication complex | positive-strand RNA virus

Significance

Hepatitis E virus (HEV) infection represents a global health challenge. However, knowledge of the viral life cycle and of the host factors required for productive infection remains limited. A genome-wide CRISPR/Cas9 screen identified Rab5A, a master regulator of early endosome biogenesis, as host factor of HEV replication. Functional and imaging studies pointed to a role of Rab5A and early endosomal membranes in HEV RNA replication, likely by serving as a scaffold for the establishment of a functional replication complex. Our findings yield insights into the life cycle of HEV, a major cause of acute hepatitis and jaundice worldwide.

Hepatitis E virus (HEV) is a major cause of acute hepatitis worldwide (1, 2). It has been classified in the *Hepeviridae* family and most human pathogenic strains belong to species *Paslahepevirus balayani* (3) which comprises eight genotypes (HEV1–8). HEV-1 to -4 represent the most important human pathogens. HEV-1 and -2 are found only in humans and are transmitted via the fecal-oral route, mainly through contaminated drinking water in resource-limited settings. HEV-3 and -4 cause zoonotic infections and are transmitted to humans primarily via the consumption of undercooked or raw pork or game meat in middle- and high-income areas. Although infection is generally self-limited, HEV-3 can persist in immunocompromised patients and lead to chronic hepatitis as well as cirrhosis (1, 2). Moreover, HEV-3 can cause neurological complications, such as neuralgic amyotrophy as well as the Guillain–Barré syndrome (4), and HEV1–4 can trigger acute-on-chronic liver failure in patients with preexisting liver disease. Hence, HEV infection is considered a global health challenge.

HEV has a 7.2-kb positive-strand RNA genome harboring three open reading frames (ORF), including ORF1 which encodes the proteins required for viral RNA replication (the so-called replicase), ORF2 which encodes the viral capsid, and ORF3 which encodes a small, palmitoylated protein required for virion secretion (5–7). As all positive-strand RNA viruses, HEV is believed to replicate its genome in a membrane-associated replication complex composed of viral proteins, notably the ORF1 protein, replicating RNA, altered cellular membranes, and other host factors (8). However, despite growing awareness and interest in hepatitis E, current understanding of the HEV life cycle is limited and the site as well as the composition of the HEV replication complex are still poorly characterized (9, 10).

Advances in CRISPR/Cas9 technology, including the development of pooled knockout (KO) libraries targeting the entire human genome, offer unprecedented opportunities to study virus–host interactions. Such libraries are designed to allow the identification of high-confidence hits by the inclusion of multiple single guide RNAs (sgRNAs) against each gene. Genome-wide CRISPR/Cas9 screens have been mainly used to study cytolytic viruses, allowing for convenient selection of virus-resistant cells and the identification of

Author affiliations: [a]Division of Gastroenterology and Hepatology, Lausanne University Hospital and University of Lausanne, Lausanne 1011, Switzerland

Author contributions: N.O., M.A., D.M., and J.G. designed research; N.O., N.D.S., and M.A. performed research; N.O. contributed new reagents/analytic tools; N.O., N.D.S., M.A., D.M., and J.G. analyzed data; and N.O., D.M., and J.G. wrote the paper.

The authors declare no competing interest.

This article is a PNAS Direct Submission.

[1]To whom correspondence may be addressed. Email: darius.moradpour@chuv.ch or jerome.gouttenoire@chuv.ch.

This article contains supporting information online at https://www.pnas.org/lookup/suppl/doi:10.1073/pnas.2307423120/-/DCSupplemental.

Published December 18, 2023.

host factors required for virus entry, genome translation, replication, or virus-induced cell death (11–14).

Here, we developed subgenomic HEV replicons allowing for positive and negative selection to perform a genome-wide CRISPR/Cas9 screen for host factors of HEV RNA replication. This approach combined with siRNA-mediated silencing and pharmacological inhibition as well as imaging studies revealed a role for Rab5A and early endosomes in HEV RNA replication, likely by serving as a scaffold for the establishment of a functional replication complex.

Results

A Genome-Wide CRISPR/Cas9 Screen Identifies Host Factors of HEV Replication. To identify host factors required for HEV replication, we performed a genome-wide CRISPR/Cas9 screen using an sgRNA library (15). As HEV is not cytopathic in cell culture, we developed an HEV-3 "suicide replicon", namely HEV83-2_TK-Neo, which can induce cell death when replicating. This construct, prepared on the basis of a previously described Gluc replicon (16), allows expression of the herpes simplex virus thymidine kinase (HSV-TK) and of the neomycin phosphotransferase II (Neo) fused by a self-cleaving P2A peptide (Fig. 1*A*). Hence, HEV RNA-replicating cells can, on the one hand, be selected by G418 treatment and, on the other hand, be killed by the addition of ganciclovir (GCV) which is metabolized by HSV-TK into a toxic triphosphate.

In order to assess functionality of the HSV-TK-P2A-Neo (TK-Neo) fusion construct and to set up the screening conditions, Huh-7.5 cells electroporated with HEV83-2_TK-Neo or HEV83-2_Neo RNA as control were first subjected to treatment with G418 for 5 d (Fig. 1*B*). As shown in Fig. 1*C*, a very similar cell survival rate of about 60% was observed for both constructs, indicating that the TK-Neo fusion construct can confer resistance to G418. Subsequently, cells were subjected to treatment with GCV for 5 d in order to assess functionality of TK (Fig. 1*B*). As shown in Fig. 1*C*, cells transfected with the HEV83-2_TK-Neo replicon died massively, i.e., >95 %, while no mortality was observed in cells transfected with HEV83-2_Neo despite very similar replication kinetics for both replicons (Fig. 1*D*). Hence, HSV-TK and Neo are fully functional in the context of a fusion construct expressed from a subgenomic HEV replicon, building the basis for a genome-wide CRISPR/Cas9 screen.

Screens were performed in Huh-7.5 human hepatocellular carcinoma cells which have been used successfully in other CRISPR/Cas9 screens (12, 17, 18). In our TK-Neo screen, Huh-7.5 cells were first electroporated with either HEV83-2_TK-Neo or HEV83-2_Neo RNA as control, followed by selection with G418

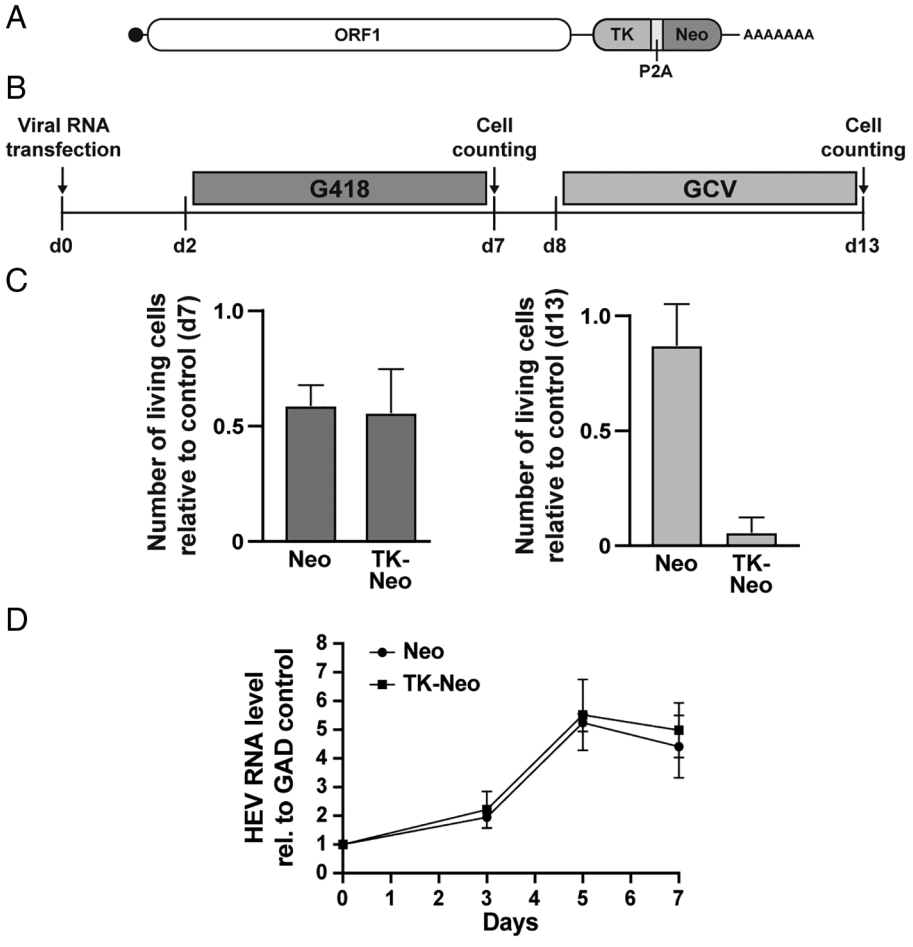

Fig. 1. Subgenomic HEV replicon allowing for positive and negative selection. (*A*) Schematic representation of subgenomic HEV replicon HEV83-2_TK-Neo used in the genome-wide CRISPR/Cas9 screen ("TK-Neo screen"). Neo, neomycin phosphotransferase II; ORF1, HEV open reading frame 1; P2A, self-cleaving 2A peptide from porcine teschovirus-1; TK, herpes simplex virus thymidine kinase. (*B*) Huh-7.5 cells were electroporated with HEV83-2_TK-Neo or HEV83-2_Neo RNA. Two days post-electroporation, cells were treated or not with 400 μg/mL geneticin (G418) for 5 d, followed by counting of surviving cells. Cells were subsequently treated or not with 2 μM ganciclovir (GCV) for 5 d, followed by counting of surviving cells. (*C*) Histograms show the number of viable cells relative to untreated control cells after G418 (*Left*; day 7) or GCV (*Right*; day 13) treatment. (*D*) Huh-7.5 cells transfected with HEV83-2_TK-Neo, HEV83-2_Neo, or HEV83-2_GAD construct, were analyzed at day 3, 5, and 7 post-transfection by quantitative RT-PCR. RNA levels are expressed relative to GAD control. Error bars represent mean ± SDs.

(Fig. 2*A*). Next, selected cells were transduced with lentiviruses expressing the GeCKO v2 human CRISPR KO library targeting 19,050 genes with 6 sgRNAs per gene (15), followed by selection with puromycin. Finally, cells were treated with GCV to select for replication-incompetent cells from which genomic DNA was harvested for next-generation sequencing (Fig. 2*A*).

Model-based analysis of genome-wide CRISPR/Cas9 knockout (MAGeCK) analysis allowed to rank the most significant hits by comparing the repertoire of sgRNAs found in HEV83-2_TK-Neo vs. HEV83-2_Neo cell populations after GCV selection (19). Bioinformatic analyses of the data did not allow to identify a particular cluster or a family of proteins among the most significant hits. Of note, the top hit of the TK-Neo screen was Golgi brefeldin A resistant guanine nucleotide exchange factor 1 (GBF1) (Fig. 2*B*), which had been identified as host factor for HEV replication in a previous targeted study (20).

In parallel to the principal TK-Neo screen, we conducted an independent screen using an HEV replicon expressing only HSV-TK (HEV83-2_TK). In this complementary TK screen, we first transduced Huh-7.5 cells with the GeCKO v2 library and selected KO cells by puromycin, followed by two rounds of HEV83-2_TK electroporation and GCV treatment (*SI Appendix*, Fig. S1). This experimental design, which may favor the identification of host factors involved in the early steps of HEV RNA replication, confirmed several hits identified as common in the top 20 candidates of both screens (Table 1).

Validation of the 20 top hits from the TK-Neo screen was performed by assessment of HEV RNA replication in Huh-7.5 cells electroporated with HEV83-2_Gluc and transfected with pools of siRNAs targeting each of the candidate genes. Luciferase activity and cell viability were assessed at day 5 post-electroporation. As shown in Fig. 2*C*, Rab5A was one of the most promising candidates when considering the degree of reduction of HEV RNA replication and a cell viability threshold at 75% of the control. Of note, Rab5A, which has been further validated by individual siRNA-mediated knockdown (*SI Appendix*, Fig. S2), was also one of the top hits in the independent TK screen (Table 1 and *SI Appendix*, Fig. S1).

Rab5A Partially Colocalizes with the HEV ORF1 Protein. Rab5A is a small GTPase involved in intracellular membrane trafficking and, more specifically, in the fusion of early endosomal

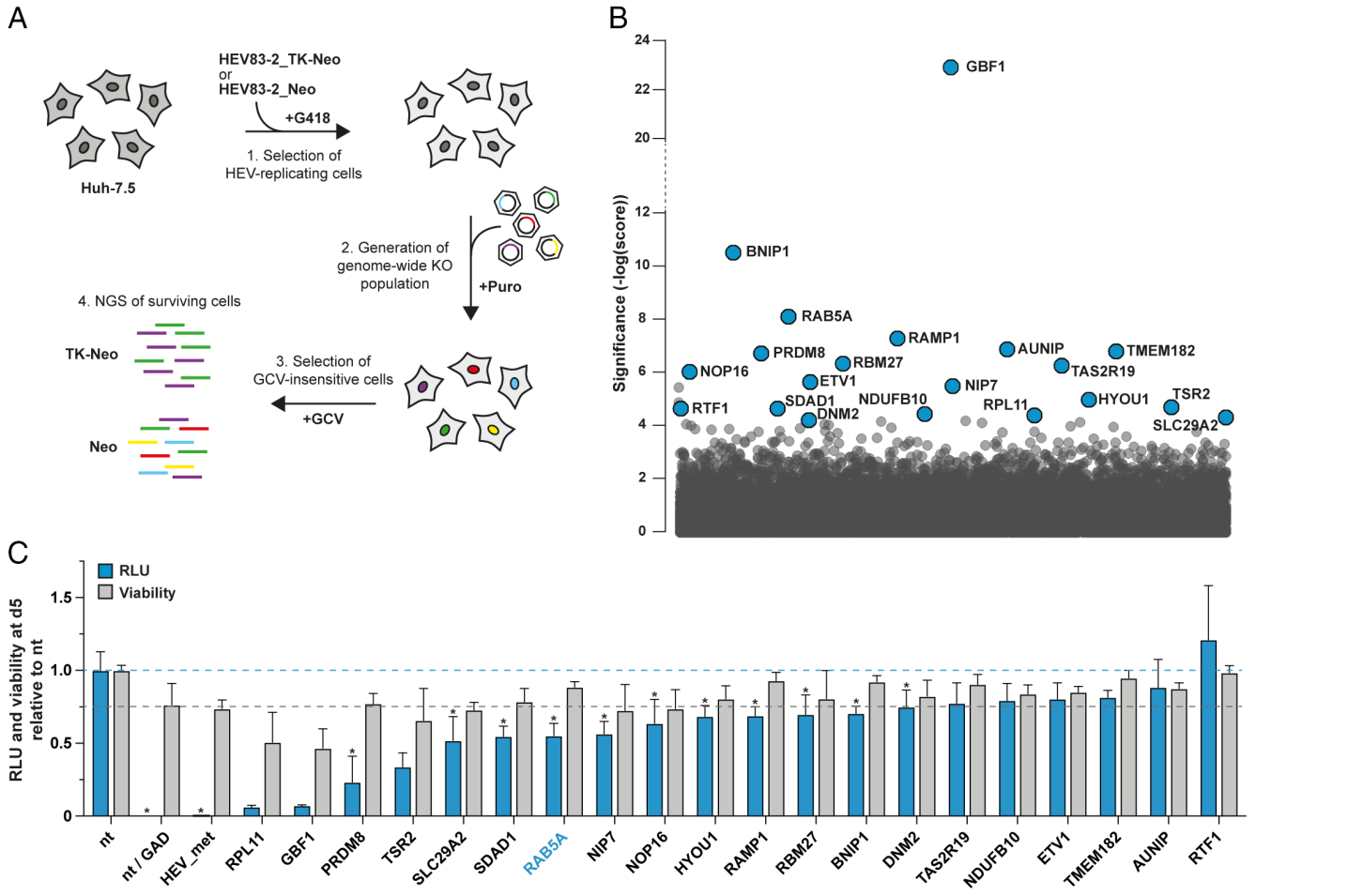

Fig. 2. Genome-wide CRISPR/Cas9 screen identifies host factors critical for HEV replication. (*A*) Genome-wide CRISPR/Cas9 screen workflow (TK-Neo screen; please refer to *SI Appendix*, Fig. S1 for "TK screen"). 1) Huh-7.5 cells were electroporated with in vitro transcribed replicon RNA, either HEV83-2_TK-Neo or HEV83-2_Neo, followed by selection with 400 μg/mL geneticin (G418) for 5 d. 2) The selected G418-resistant cells, from both populations, were transduced with lentiviruses harboring GeCKO v2 libraries A or B at a multiplicity of infection of 0.3, followed by selection with 5 μg/mL puromycin (Puro) for an additional 5 d. 3) Finally, both cell populations, referred to as "TK-Neo" and "Neo", were treated with 2 μM ganciclovir (GCV) for 5 d, 4) followed by extraction of genomic DNA and next-generation sequencing (NGS). (*B*) Results of the genome-wide CRISPR/Cas9 screen as analyzed by the model-based analysis of genome-wide CRISPR/Cas9 knockout (MAGeCK) tool. The screen was performed in two replicates. The 20 most enriched genes are colored in blue. (*C*) Validation of the 20 top candidates. Huh-7.5 cells were electroporated with reporter replicon HEV83-2_Gluc or the replication-deficient control HEV83-2_Gluc-GAD (GAD). On the same day and again on day 3, cells were transfected with pools of siRNAs targeting each of the top 20 hits. An siRNA targeting the HEV ORF1 methyltransferase domain (HEV_met) was used as a control for transfection efficiency. Luciferase activity as well as cell viability were determined at day 5 and are represented by histograms with a normalization to non-targeted control siRNA (nt). The asterisk (*) indicates statistically significant differences with $P < 0.05$.

Table 1. MAGeCK results of the genome-wide CRISPR/Cas9 screens performed with subgenomic HEV replicons HEV83-2_TK-Neo (TK-Neo screen) and HEV83-2_TK (TK screen)

	TK-Neo screen (n = 2)			TK screen (n = 3)		
Rank	Gene	Score	*P*-value	Gene	Score	*P*-value
1	*GBF1*	1.26e-23	2.42e-7	*CD63*	2.65e-9	2.42e-7
2	*BNIP1*	2.92e-11	2.42e-7	***RAB5A***	1.10e-7	1.69e-6
3	***RAB5A***	7.12e-9	2.42e-7	***TAS2R19***	3.44e-5	1.33e-4
4	***RAMP1***	4.818-8	2.42e-7	***RAMP1***	3.98e-5	1.83e-4
5	***AUNIP***	1.26e-7	1.69e-6	***AUNIP***	3.99e-5	2.24e-4
6	***TMEM182***	1.51e-7	2.18e-6	***TMEM182***	5.16e-5	2.82e-4
7	***PRDM8***	1.78e-7	2.66e-6	***RBM27***	5.56e-5	3.02e-4
8	***RBM27***	4.33e-7	4.11e-6	***PRDM8***	5.69e-5	3.10e-4
9	***TAS2R19***	5.26e-7	5.07e-6	*METTL11B*	9.62e-5	5.16e-4
10	*NOP16*	8.73e-7	8.94e-6	*IPO9*	1.21e-4	6.61e-4
11	*ETV1*	2.15e-6	1.47e-5	*TTC16*	1.30e-4	7.09e-4
12	*NIP7*	2.96e-6	2.30e-5	*RNASE9*	1.33e-4	7.24e-4
13	*HYOU1*	9.83e-6	6.74e-5	*LRRC18*	1.36e-4	7.45e-4
14	*TSR2*	1.84e-5	1.09e-4	*LGR5*	1.80e-4	9.95e-4
15	*RTF1*	2.08e-5	1.20e-4	*COL24A1*	1.81e-4	1.01e-3
16	*SDAD1*	2.09e-5	1.21e-4	*LLGL1*	1.86e-4	1.04e-3
17	*NDUFB10*	3.34e-5	1.91e-4	*FAM122B*	1.99e-4	1.10e-3
18	*RPL11*	3.78e-5	2.15e-4	*CCSER2*	2.09e-4	1.14e-3
19	*SLC29A2*	4.55e-5	2.54e-4	*PPAPDC3*	2.25e-4	1.22e-3
20	*DNM2*	5.72e-5	3.11e-4	*SEPT14*	2.26e-4	6.71e-4

"Score" corresponds to the robust ranking aggregation (RRA) lo value of the given gene in positive selection. *P*-value" is the raw *P*-value of the given gene in positive selection. Candidate genes identified among the top 20 hits in both screens are highlighted in bold. *n* denotes the number of replicates of the screens.

membranes (21–23). In addition to wt Rab5A, we investigated the functionally impaired mutants Rab5A_Q79L and Rab5A_S34N. Rab5A_Q79L has deficient GTPase activity, resulting in continuous membrane fusion and the formation of large vesicles with characteristics of both early and late endosomes (24). Rab5A_S34N is a dominant-negative mutant resulting in impaired endosomal membrane fusion (25). Monitoring of an HEV Gluc replicon in Huh-7.5 cells overexpressing wt Rab5A or the two mutants revealed similar levels of HEV RNA replication in this transient setting (Fig. 3*A*), including when endogenous Rab5A expression is silenced and siRNA-resistant Rab5A constructs are overexpressed (*SI Appendix*, Fig. S3).

Both endogenous Rab5A and the HEV ORF1 protein (corresponding to the viral replicase) are expressed at low levels and are difficult to detect by immunofluorescence microscopy. Hence, we developed mCherry-tagged versions of wt Rab5A as well as the two mutants and expressed these after lentiviral cell transduction. In addition, we took advantage of recently developed subgenomic HEV replicons and full-length genomes harboring a hemagglutinin (HA) tag in the ORF1 protein, enabling detection of the replicase by immunofluorescence (16). Of note, Hep293TT human hepatoblastoma cells were used for these investigations as they offered the best detection of the ORF1 protein required for colocalization experiments.

As shown in Fig. 3 *B* and *C*, wt Rab5A (Rab5A_wt), Rab5A_Q79L, and Rab5A_S34N partially colocalized with the ORF1 protein expressed from subgenomic HEV replicon RNA (HEV83-2_Gluc_B2HA), with a mean Pearson's coefficient ± SD of 0.58 ± 0.07 in cells harboring Rab5A_wt and HEV83-2_Gluc_B2HA (Fig. 3*C*, first scatter blot).

In line with the replication data (Fig. 3*A*), partial colocalization of ORF1 protein and Rab5A was also observed for mutants Q79L (mean Pearson's coefficient ± SD 0.67 ± 0.08) and S34N (mean Pearson's coefficient ± SD 0.61 ± 0.08) despite the formation of very large and small endosomes, respectively (Fig. 3 *B* and *C*). Of note, colocalization of the ORF1 protein and Rab5A is significantly enhanced in the Q79L mutant in the subgenomic HEV replicon RNA settings (Fig. 3*C*), reflecting improved visualization of the replicase and, thereby, of likely replication complexes on the large endosomal structures induced by this mutant. Interestingly, very similar results were obtained with a full-length HEV construct (Fig. 3*C* and *SI Appendix*, Fig. S4), albeit with significantly lower mean Pearson's coefficients ± SD (0.58 ± 0.07 vs. 0.48 ± 0.08) in cells harboring Rab5A_wt and HEV83-2_Gluc_B2HA vs. HEV83-2_B2HA constructs; P = 0.0152) likely reflecting the involvement of ORF1 protein in additional functions which are operative only in the full-length context, e.g., virion assembly or release, as suggested earlier (26).

Taken together, these results suggest that the ORF1 protein, corresponding to the HEV replicase, localizes to the same subcellular compartment as Rab5A independently of the latter's capacity to mediate endosomal membrane fusion.

Early Endosomes Are Involved in HEV RNA Replication. The functional and imaging data above, i.e., the reduction of HEV RNA replication by silencing of Rab5A and the partial colocalization of ORF1 protein with Rab5A, point toward a role of early endosomes in HEV RNA replication. To validate and extend these observations, we assessed the replication of subgenomic replicon HEV83-2_Gluc in Huh-7.5 cells transfected with siRNAs against EEA1 (early endosome antigen 1) and APPL1 (adaptor protein containing a PH domain, a PTB domain and a leucine zipper motif 1), two partners of Rab5A, against the late endosome component Rab7A, against the recycling endosome

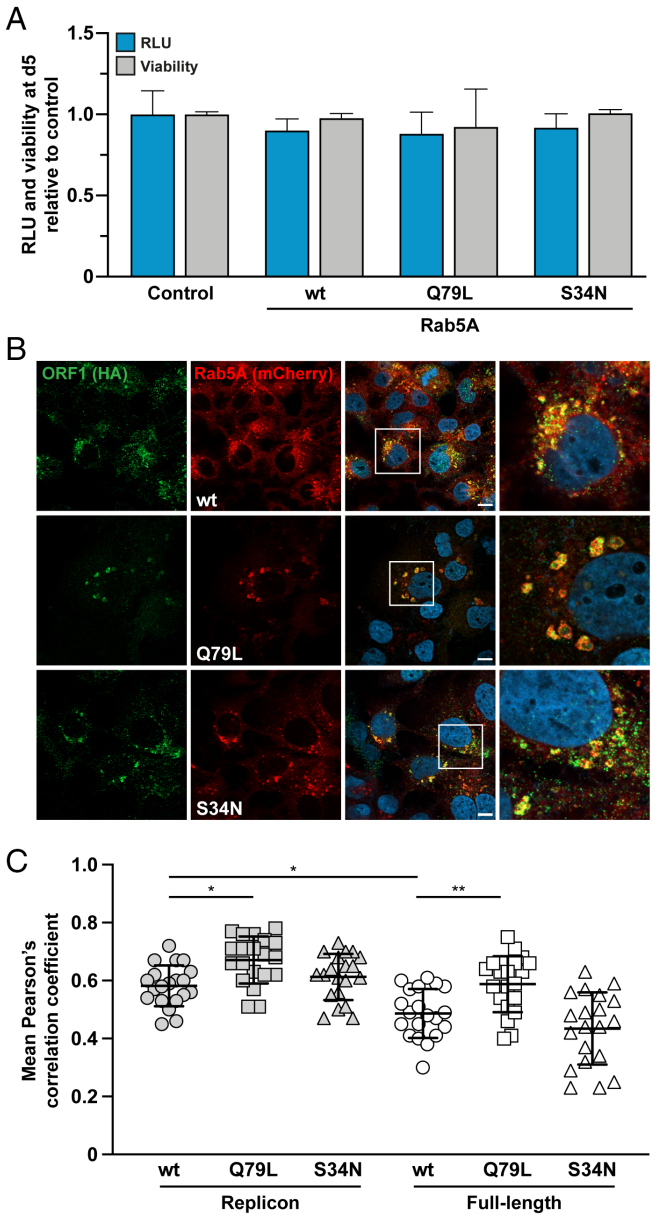

Fig. 3. Rab5A partially co-localizes with the HEV ORF1 protein. Huh-7.5 cells were transduced with lentiviruses expressing Rab5A as well as Q79L and S34N mutants (pWPI-RAB5A, pWPI-RAB5A_Q79L, pWPI-RAB5A_S34N, respectively), followed 2 days later by selection with 3 μg/mL blasticidin for 8 d. (*A*) Selected cells were electroporated with subgenomic reporter replicon HEV83-2_Gluc and luciferase activity as well as cell viability were determined 5 d later. Results are represented by histograms and shown as relative light units (RLU) normalized to replication in cells transduced with an empty vector (Control). (*B*) Hep293TT transduced cells were electroporated with HEV83-2_B2HA-Gluc RNA, fixed 6 d post-electroporation, subjected to immunofluorescence using rabbit mAb C29F4 against the HA tag and analyzed by confocal laser scanning microscopy. Nuclei were counterstained with DAPI (blue) and white squares indicate areas shown at higher magnification on the right row. The scale bar represents 10 μm. (*C*) Mean Pearson's correlation coefficients were determined for each condition ($n \geq 20$ cells each). The same experiment was performed with subgenomic replicon HEV83-2_B2HA-Gluc (panels *A* and *B* as well as *Left* part of panel *C* [Replicon]) and with the full-length construct HEV83-2_B2HA (*Right* part of panel *C* [Full-length]). The lines indicate means ± SDs. Statistical differences are denoted by * for $P \leq 0.05$ and ** for $P \leq 0.01$.

component Rab11A, and against CD63, a tetraspanin present along the entire endosomal pathway (27). Immunoblot confirmed efficient silencing of the respective targets (*SI Appendix*, Fig. S5).

Silencing of Rab5A as well as of its companion early endosome components EEA1 and APPL1 reduced HEV RNA replication significantly and to a similar degree both in cells harboring the HEV-3 clones, i.e., 83-2 or Kernow-C1 p6, and HEV-1 clone Sar55 (Fig. 4*A* and *SI Appendix*, Fig. S6). Silencing of the late endosome marker Rab7A and of the recycling endosome marker Rab11A did not affect replication of the 83-2 clone but enhanced replication of the p6 clone, as well as of the Sar55 clone for Rab7A silencing (Fig. 4*A* and *SI Appendix*, Fig. S6), suggesting that replication is favored when maturation or recycling of the early endosomes is slowed down. Interestingly, silencing of CD63, which had been identified as the top candidate in the TK screen (Table 1 and *SI Appendix*, Fig. S1), reduced HEV RNA replication to a degree similar to that of the early endosome components Rab5A, EEA1, and APPL1, in line with the requirement of the endosomal pathway for viral replication. Cell viability was unaffected by transfection of the different siRNAs.

As a complementary approach to siRNA-mediated gene silencing, we employed pharmacological inhibitors to assess the role of early endosomes in HEV RNA replication. To this end, Huh-7.5 cells electroporated with subgenomic replicon HEV83-2_Gluc were treated with the Rab5A inhibitor neoandrographolide (NAP) (28) or the dynamin inhibitors Dyngo4a and Dynasore (29, 30). Dynamin-2, which fuels early endosomes with membranes originating from the plasma membrane, was also identified in the TK-Neo screen as well as validated as a host factor (Fig. 2*B* and 2*C* as well as Table 1). As shown in Fig. 4*B*, NAP, Dyngo4a and Dynasore inhibited HEV RNA replication in a dose-dependent manner without affecting cell viability under the given experimental condition. This dose-dependent inhibition of replication by NAP, Dyngo4a, and Dynasore was confirmed in the human hepatoblastoma Hep293TT cells (*SI Appendix*, Fig. S7). The effect of the dynamin inhibitors could be confirmed in cells infected with cell culture–derived HEV. However, NAP, which had a modest impact in the replication assay, did not show any significant effect in an infection setting (Fig. 4*C*). To further investigate the importance of early endosomes, the PIKfyve inhibitor apilimod (31), which inhibits the synthesis of phosphatidylinositol 3,5-bisphosphate required for maturation of early endosomes, was evaluated with the Gluc subgenomic replicon. As expected, PIKfyve inhibition by apilimod increased HEV replication (Fig. 4*D*). Together, these data support a role of early endosomal membranes in HEV RNA replication.

Replicating HEV RNA Localizes to Early Endosomes. To further address a role of early endosomal membranes in HEV RNA replication, we investigated Rab5A and HEV ORF1 protein together with viral positive- and negative-strand RNA in cells replicating a full-length HEV genome. To this end, Hep293TT cells expressing mCherry-tagged wt Rab5A or the Rab5A mutant Q79L were electroporated with full-length RNA derived from the HEV-3 p6 clone harboring an HA tag in the ORF1 protein (HEVp6_HA) and analyzed at day 3 post-transfection by immunofluorescence for HA-tagged ORF1 protein coupled with FISH for positive- and negative-strand HEV RNA (Fig. 5*A*).

Rab5A and HEV ORF1 protein are detected together with the viral positive-strand RNA. Localization of HEV positive-strand RNA to endosomes can be appreciated particularly well in the large endosomes induced by Rab5A_Q79L (Fig. 5*A*), although weighted colocalization coefficients were found to be similar for wt Rab5A and Q79L mutant, i.e., 0.66 ± 0.2 and 0.60 ± 0.25, respectively (Fig. 5*B*). Similar observations were also made at day 6, when viral particles are produced (*SI Appendix*, Fig. S8), with weighted colocalization coefficients of 0.71 ± 0.19 and 0.67 ± 0.26, respectively (Fig. 5*B*). Findings are consistent for HEV clones 83-2 and p6, with a stronger FISH signal for the latter due

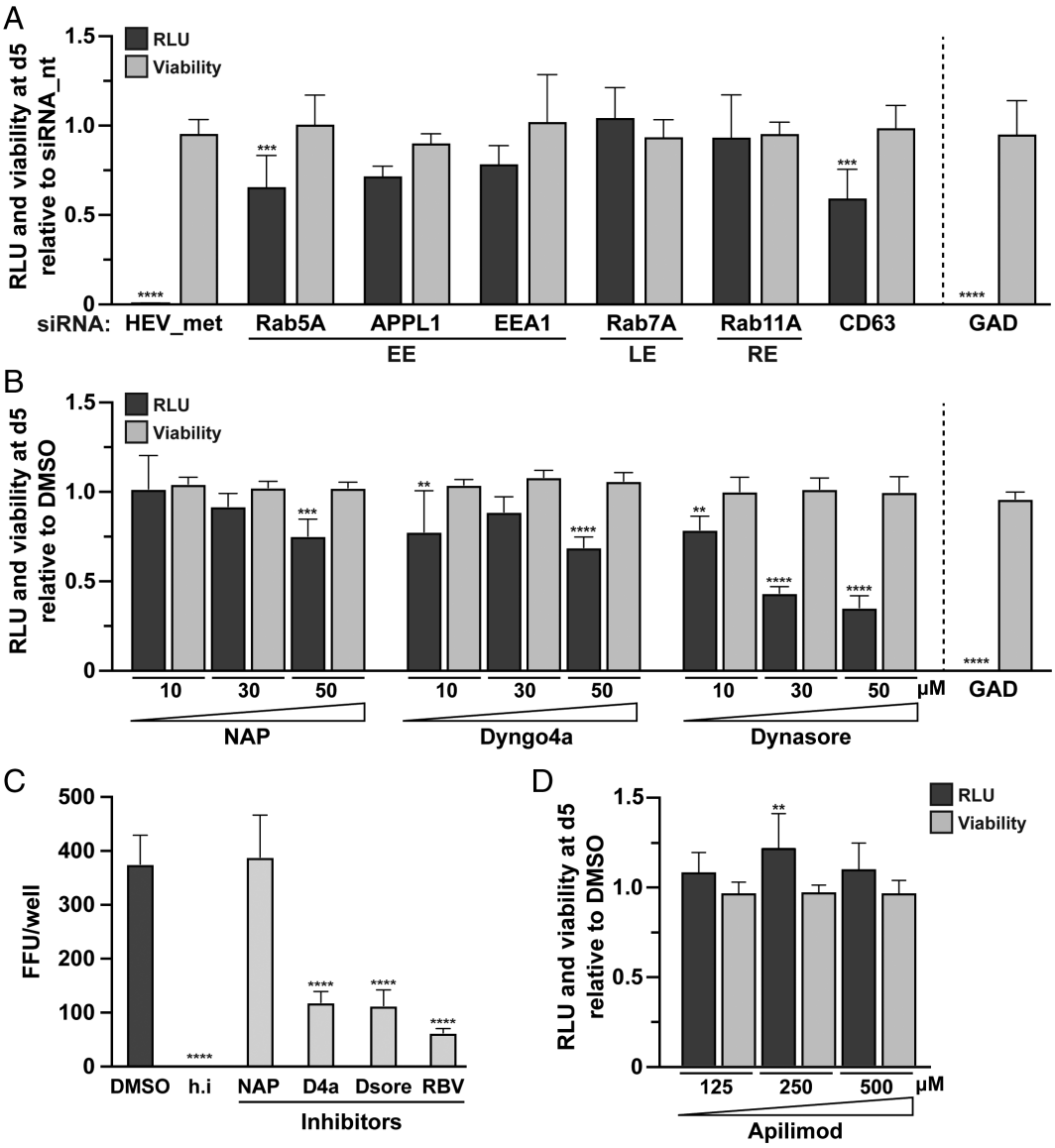

Fig. 4. A role for early endosomes in HEV replication. (*A*) Huh-7.5 cells were electroporated with reporter replicon HEV83-2_Gluc or the replication-deficient control HEV83-2_Gluc-GAD (GAD). On the same day and on day 3 post-electroporation, cells were transfected with pools of siRNAs targeting early endosome (EE) components Rab5A, APPL1, and EEA1, late (LE) and recycling endosome (RE) components Rab7A and Rab11A, respectively, as well as CD63. An siRNA targeting the HEV ORF1 methyltransferase domain was used as a control for transfection efficiency (HEV_met). Luciferase activity and cell viability were determined on day 5 and are represented by histograms with a normalization to non-targeting (nt) siRNA. Statistical differences compared to nt are denoted by ** for $P \leq 0.01$, *** for $P \leq 0.001$, and **** for $P \leq 0.0001$. (*B*) Huh-7.5 cells were electroporated with reporter replicon HEV83-2_Gluc or the replication-deficient control HEV83-2_Gluc-GAD (GAD). On day 3 post-electroporation, cells were treated with neoandrographolide (NAP), Dyngo4a, or Dynasore at concentrations of 10, 30, and 50 µM. Luciferase activity and cell viability were determined at day 5 and are represented by histograms with normalization to carrier (DMSO) treated cells. Statistical differences compared to DMSO are denoted by ** for $P \leq 0.01$, *** for $P \leq 0.001$ and **** for $P \leq 0.0001$. (*C*) Huh-7.5 cells were infected with cell culture–derived HEV from the p6 clone and treated, 1 d later, for 2 d with 50 µM of NAP, Dyngo4a (D4a), Dynasore (Dsore), or ribavirin (RBV). The number of infection events was determined by focus forming assay at day 3 post-infection and shown as focus forming units (FFU) per infected well. DMSO-treated cells served as reference and a heat-inactivated inoculum (h.i.) served as negative control. Statistical differences compared to the DMSO reference are denoted by **** for $P \leq 0.0001$. (*D*) In a similar manner as in panel (*B*), Huh-7.5 cells electroporated with the HEV83-2_Gluc replicon were treated with 125, 250, and 500 µM of apilimod, and luciferase activity was measured at day 5. Statistical differences compared to the DMSO reference are denoted by ** for $P \leq 0.01$.

to optimal complementarity with the probes that had been designed for this clone (*SI Appendix*, Fig. S9). The HEV negative-strand RNA, pointing more specifically to the site of viral RNA replication, is detected together with ORF1 protein and Rab5A, especially at the vicinity of Q79L-induced large endosomes (Fig. 5*A* and *SI Appendix*, Fig. S8). Image analyses confirmed that Rab5A wt and Q79L are colocalizing with negative-strand HEV RNA, as indicated by weighted colocalization coefficients of 0.76 ± 0.24 and 0.75 ± 0.23, respectively (Fig. 5*B*). This strong colocalization is also observed at day 6 post-transfection (Fig. 5*B* and *SI Appendix*, Fig. S6). Specificity of the FISH signal for both RNA species was confirmed by electroporation and analysis of a replication-deficient (GAD) HEV genome (*SI Appendix*, Fig. S10).

Taken together, these results indicate that HEV RNA replication takes place at early endosomal membranes.

Discussion

Despite hepatitis E being clinically more recognized, current understanding of the HEV life cycle and of the host factors required for productive infection remains limited. Here, we

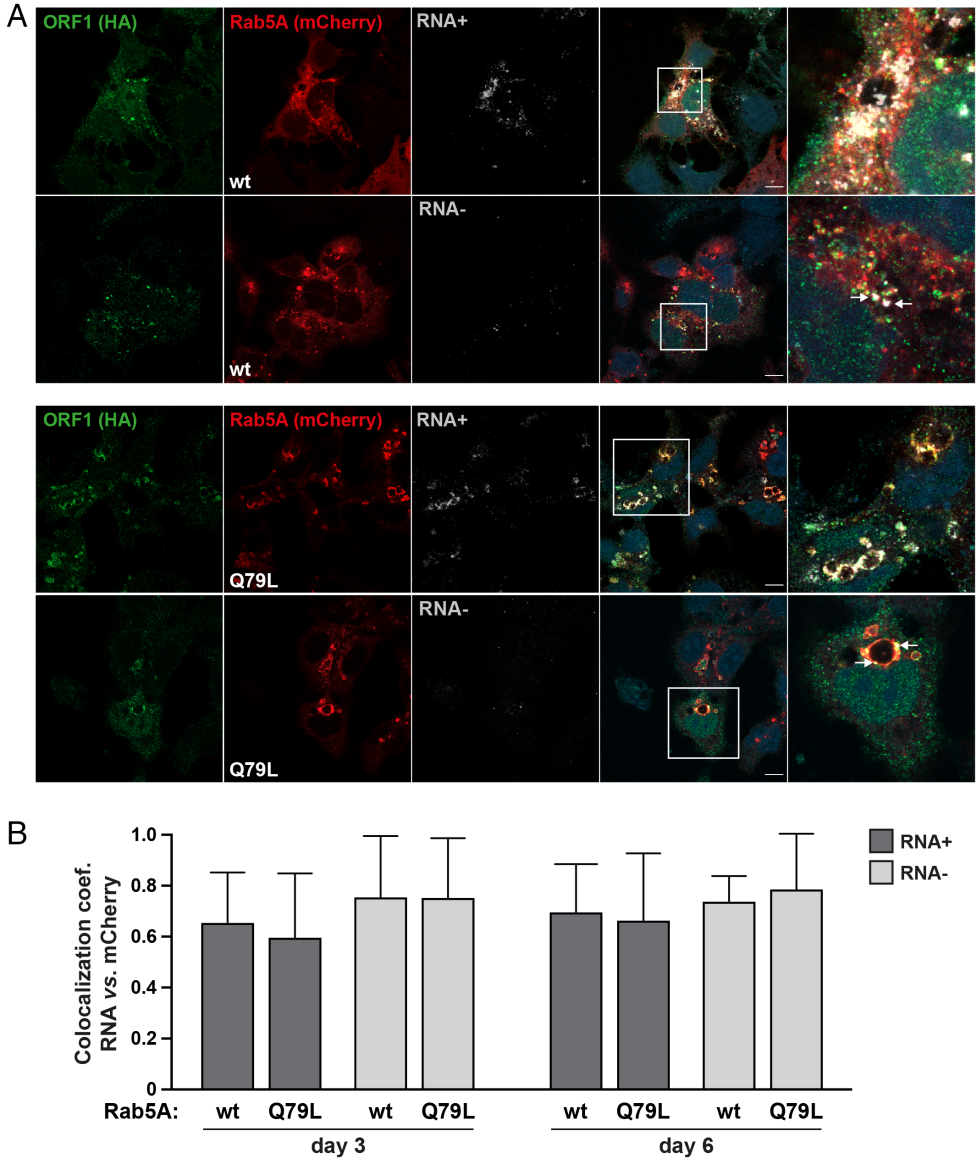

Fig. 5. Colocalization of Rab5A, ORF1 protein, and viral positive- as well as negative-strand RNA in cells replicating a full-length HEV genome. (*A*) Hep293TT cells overexpressing wild-type Rab5A (wt) or mutant Rab5A Q79L (Q79L) fused to mCherry were electroporated with full-length HEVp6_HA RNA, fixed at day 3 post-electroporation and subjected to fluorescence in situ hybridization using HEV-specific probes for the detection of positive-strand RNA [RNA+] (probe V-HEV-p6-ORF1-O2-C2) or negative-strand RNA [RNA−] (probe V-HEV-p6-ORF2-sense-C3), followed by immunofluorescence detection of HA-tagged ORF1 protein using rabbit monoclonal antibody C29F4 against the hemagglutinin (HA) tag. Nuclei were counterstained with DAPI (blue) and white squares indicate areas shown at higher magnification on the *Right*. Arrows indicate negative-strand RNA. The scale bar represents 10 μm. (*B*) Weighted colocalization coefficients of RNA vs. mCherry signals were determined using the Zeiss ZEN Blue software ($n \geq 9$ cells for each condition) and represented by histograms showing mean ± SD. Results from panel (*A*) as well as from *SI Appendix*, Fig. S8 were analyzed.

developed and exploited subgenomic replicons allowing for positive and negative selection (suicide replicons) to perform a genome-wide CRISPR/Cas9 screen for host factors of HEV RNA replication. Two different screens were performed, a TK-Neo screen, involving positive selection of cells harboring replicating HEV RNA in a first step and elimination (negative selection) of such cells in a second step, and a TK screen, involving the direct elimination of viral RNA replicating cells. Both screens yielded a number of significant hits including Rab5A, a small GTPase regulating early endosome trafficking and fate, which was further characterized in the present study.

Congruent results obtained in HEV-3 clones 83-2 (32) and Kernow-C1 p6 (33) as well as in HEV-1 clone Sar55 (34) demonstrated that silencing of Rab5A expression significantly decreases HEV RNA replication. Functional interference with key components of the endosomal pathway as well as colocalization of the HEV ORF1 protein, representing the viral replicase, with Rab5A and viral positive- and negative-strand RNAs revealed a role for early endosomal membranes in HEV replication.

As HEV does not display any intrinsic cytopathic effect in current cell culture models, we prepared suicide replicons expressing HSV-TK, allowing to eliminate (negatively select) cells harboring replicating viral RNA upon GCV treatment. HSV-TK has been widely employed as a suicide gene to eliminate cancer cells targeted by gene therapy (35). Fusion constructs composed of HSV-TK and Neo have previously been shown to be functional, albeit at reduced efficacy (36). Hence, we inserted a P2A peptide between the two moieties, enabling their function as individual enzymes upon self-cleavage. Although indirect cell death–inducible systems based on the NS3-4A protease activity have been designed to

identify HCV antiviral drugs or host factors (37, 38), so far, this "suicide" strategy, including GCV-induced cell death, has been rarely employed in virology. Hence, our study represents a proof-of-concept that may be potentially applied to other noncytopathic viruses.

Our screens revealed candidates playing a role in membrane formation and trafficking such as Rab5A, CD63, and dynamin-2, known to be involved in infection by other viruses (39–41), but also the SNARE endoplasmic reticulum-to-Golgi anterograde transport protein BNIP1 (BCL2 interacting protein 1) and GBF1 which interfere with cellular membrane homeostasis. Interestingly, among the few host factors of HEV replication described to date (9, 10), GBF1 has previously been identified by a directed approach (20), thereby validating our unbiased screening strategy.

GBF1, known to activate different ADP-ribosylation factor proteins to regulate cellular vesicular transport, more specifically the COPI vesicle transport (42), has been found to be involved in the life cycle of different RNA viruses, including in genome replication, assembly, and release. In the case of HEV, it has been shown to play a critical role in Brefeldin A–mediated inhibition of viral replication (20). Interestingly, GBF1 was a highly significant hit in our TK-Neo screen but was not identified in the TK screen. Differences in the experimental design may favor the identification of host factors involved in the establishment of viral replication in the TK screen as opposed to host factors involved throughout HEV RNA replication and possibly the persistence of viral replication in the TK-Neo screen. Of note, heat shock protein 90 (Hsp90), another previously identified host factor of HEV RNA replication (43, 44), was not in the top 20 candidates but found among the top 10% of our TK-Neo screen.

Our findings indicate that Rab5A may function as regulator of HEV replication via its role in homeostasis of the endosomal pathway. Indeed, silencing of Rab5A led to a significant decrease of replication, albeit without complete inhibition, similarly to what was observed after pharmacological inhibition of Rab5 by NAP, a compound that specifically prevents its association with GTP and GDP (28), thereby limiting the enzymatic function of Rab5A as well as interaction with partners such as EEA1 and APPL1 (Fig. 4). Accordingly, silencing of these Rab5A effectors led to a consistent decrease of HEV RNA replication. Altogether, our observations suggest that Rab5A is important but not essential for HEV RNA replication, suggesting a more general role in its regulation. Moreover, interfering with membrane supply upstream of early endosomes, by the use of inhibitors of dynamin-dependent endocytosis or silencing of dynamin-2, identified in the TK-Neo screen, decreased viral replication, thereby confirming the need for endosomal membranes to support HEV RNA replication. The importance of early endosomes is further supported by an increase in HEV replication observed after pharmacologic inhibition of phosphatidylinositol 3,5-bisphosphate synthesis, although the absence of a dose-dependent effect may result from additional consequences on early endosome composition. Finally, and in line with these observations, the dispensability of components of late (Rab7A) and recycling endosomes (Rab11A) revealed by silencing experiments suggests that blocking late maturation may be favorable to HEV RNA replication (Fig. 4 and *SI Appendix*, Fig. S6).

Overall, our data point to a role of Rab5A and endosomal membranes in HEV replication. This finding is in line with previous data on HEV egress. Indeed, it has been shown that ORF3 protein recruits a member of the endosomal sorting complex required for transport (ESCRT), Tsg101, and that their interaction is necessary for virion release (45–47). In addition, the quasi-envelope of HEV released into the bloodstream is derived from exosomes originated from late endosomes, also known as multivesicular bodies (47, 48). These features already pointed to the importance of the endosomal pathway in the HEV life cycle. The formation of a replication complex at early endosome would, therefore, connect HEV RNA replication, assembly, and release.

The subcellular localization of the HEV replicase, which has been inherently difficult to visualize in authentic replication systems, as well as the site of HEV RNA replication have not been clearly identified to date. Early studies based on heterologous ORF1 protein expression pointed to membranes of the endoplasmic reticulum or early secretory pathway (49, 50). More recently, functional HEV genomes harboring tags in the ORF1 protein allowed to localize the viral replicase expressed in a genuine replication context to cytoplasmic dot-like structures (16, 51), likely associated with membranes (16). In the present study, we provide functional evidence, through the role of Rab5A, that the early endosome compartment is key to HEV replication. Observations were consistent in different molecular clones, subgenomic and full-length replication systems, and different liver-derived cell lines, i.e., Huh-7.5 and Hep293TT cells.

In our previous study, we reported that ORF1 protein partially colocalizes with the late endosome and exosome marker CD63 (16). Here, we show that silencing of CD63 reduces HEV RNA replication. More than a marker of these late compartments, the tetraspanin CD63 originates from the plasma membrane and transits through the entire endosomal pathway (27). Interestingly, CD63 has been identified as a top hit in the TK screen but not in the TK-Neo screen likely due to the different experimental design. Until now, CD63 may have been considered to have a role in virus secretion, as it is found on quasi-enveloped HEV particles (52). However, our findings point to a role of CD63 earlier in the viral life cycle, at the step of viral RNA replication. Other viruses have been reported to depend on CD63, including at the steps of post-endocytic virion trafficking and replication, e.g., human papilloma virus or herpes simplex virus-2 (53, 54). Although the function of CD63 in the endosomal pathway is incompletely understood, it is believed to play a role in endosomal protein trafficking (55). Therefore, a role of CD63 in recruiting host factors and membranes required for the formation of the HEV replication complex is a plausible hypothesis. Further work is needed to elucidate the exact role of this tetraspanin in HEV RNA replication.

Use of cellular membranes as a scaffold for the establishment of their replication complexes is a hallmark of all positive-strand RNA viruses, allowing to concentrate important viral and host factors as well as to protect viral RNA from recognition by the innate immune system (reviewed in ref. 56). The membranes may be derived from different cellular compartments, including, among others, plasma, endoplasmic reticulum, and mitochondrial membranes. The alphaviruses, which belong to the *Togaviridae* family and include Sindbis and Semliki Forest viruses, replicate their genomes on virally induced organelles called cytopathic vacuoles (CPV) which are derived from the endosomal–lysosomal compartment (57–59). Following virus entry, uncoating, and translation of the genome, the formation of alphavirus replication complexes is likely initiated at the plasma membrane which then traffic *via* the endosomal pathway to form CPV. Hence, similarly to what is observed for other positive-strand RNA viruses and in particular for alphaviruses, it is tempting to speculate that HEV induces specific membrane rearrangements derived from early endosome to establish its replication complex. Given that our observations were made after HEV RNA transfection, thereby bypassing virus entry, and that entry of the naked HEV particle is independent of Rab5A (60), we may hypothesize that, alike alphaviruses, HEV replication complexes are present on endosomal membranes that are distinct from those employed in virion entry. Future

ultrastructural analyses shall explore these hypotheses for which our work provides a solid basis.

In conclusion, TK-based HEV replicons and a genome-wide CRISPR/Cas9 screen allowed the identification of host factors of HEV RNA replication. Rab5A and a functional endosomal pathway, in particular early endosomes, were found to have an important role in the HEV life cycle, likely in the formation of the viral replication complex. Future studies shall explore the structure and functional architecture of the HEV replication complex.

Materials and Methods

Cell Lines and Reagents. Huh-7.5 human hepatocellular carcinoma cells (61) (kindly provided by Charles M. Rice, The Rockefeller University) were maintained in Dulbecco's modified Eagle medium (DMEM) supplemented with 10% fetal bovine serum (FBS) and 0.25 mg/mL gentamicin (all from Gibco, Thermo Fischer Scientific). Hep293TT human hepatoblastoma cells (62) (kindly provided by Gail E. Tomlinson, University of Texas Health Science Center at San Antonio) were cultured in Roswell Park Memorial Institute 1640 (RPMI) medium containing HEPES buffer, 2 mM L-glutamine supplemented with 10% FBS, and 0.25 mg/mL gentamicin.

The Rab5 inhibitor neoandrographolide (NAP) was from Selleckchem, the dynamin inhibitors Dyngo4a and Dynasore from Abcam, the PIKfyve inhibitor Apilimod from MedChemExpress, and ribavirin from Sigma-Aldrich.

Antibodies. Mouse monoclonal antibody (mAb) anti-β-actin was from Sigma-Aldrich. Rabbit polyclonal antibody anti-Rab5 and mouse mAb anti-Rab7A were from Abcam. Mouse mAbs anti-Rab11A and anti-EEA1 were from R&D Systems. Mouse mAbs anti-APPL1 and anti-CD63 were from Santa Cruz. Rabbit mAb C29F4 against the HA tag was from Cell Signaling Technology. Rabbit polyclonal antibody against ORF2 was kindly provided by Rainer G. Ulrich (Friedrich Loeffler Institute). Horseradish peroxidase–conjugated anti-mouse and anti-rabbit secondary antibodies were from GE Healthcare and Agilent Technologies, respectively. Alexa® Fluor 488 anti-rabbit secondary antibodies were from Thermo Fisher Scientific.

Plasmids. Constructs were derived from the HEV-3 infectious clones 83-2-27 (referred to in the following as 83-2) (32) (Genbank accession number AB740232; kindly provided by Koji Ishii and Takaji Wakita, National Institute of Infectious Diseases) or Kernow-C1 p6 (referred to in the following as p6) (33) (Genbank accession number JQ679013; kindly provided by Suzanne U. Emerson, NIH). The HEV-1 Gaussia luciferase replicon construct derived from Sar55 clone was also used for luciferase assay (GenBank accession no. AF444002; kindly provided by Suzanne U. Emerson, NIH) (63). Primers used are listed in *SI Appendix*, Table S1. All constructs were verified by sequencing.

A subgenomic HEV replicon allowing expression of the herpes simplex virus thymidine kinase (HSV-TK) and of the neomycin phosphotransferase II (Neo) fused by a self-cleaving P2A peptide [ATNFSLLKQAGDVEENPGP] from porcine teschovirus-1 (64) was prepared by PCR amplification from HEV83-2_HSV-TK and HEV83-2_Neo (*SI Appendix*) using forward primer HSVTK-fd and P2A-Neo-fd together with reverse primers HSVTK-LinkP2A-rv and Neo-XbaI-rv, respectively (*SI Appendix*, Table S1). The PCR product from HEV83-2_HSV-TK was used as template for an additional PCR amplification using forward primer HSVTK-fd and reverse primer LinkerP2A-rv. The amplification product together with the one from HEV83-2_Neo PCR was used as template for overlap extension PCR using forward primer HSVTK-fd and reverse primer Neo-XbaI-rv. The HEV83-2_TK-Neo plasmid was then prepared by *BsrGI*-*Xba*I digestion and cloning into HEV83-2_HSV-TK.

The lentiviral Rab5A expression vector pWPI-RAB5A was prepared by PCR amplification from FLAG-Rab5A (65) (Addgene plasmid #28043; Gift from Qing Zhong) using primers pWPI-RAB5A-fd and pWPI-RAB5A-rv (*SI Appendix*, Table S1), followed by Gibson assembly (New England Biolabs) using the PCR product and *Sma*I-digested pWPI-X-FLAG (*SI Appendix*).

Preparation of Rab5A mutants, mCherry-tagged constructs, as well as HA-tagged HEV genomes are described in *SI Appendix*.

Lentivirus Production. The human GeCKO v2 CRISPR knockout library (15) (Addgene #1000000048; kindly provided by Feng Zhang, Broad Institute of MIT and Harvard) was amplified in EC100 bacteria (Epicentre) as two separate pools (library A and B). Lentiviruses were then produced as described in *SI Appendix*.

Gene Silencing. ON-TARGETplus SMARTPool siRNAs targeting the top 20 candidates of the TK-Neo screen, EEA1, APPL1, RAB7A, RAB11A, CD63, and non-targeting control siRNA were purchased from Dharmacon (Horizon Discovery). SiRNA targeting the ORF1 methyltransferase domain from HEV 83-2 or p6 clone was designed based on information kindly shared by Viet Loan Dao Thi (University of Heidelberg) (66), and its synthesis was carried out by Microsynth AG. Huh-7.5 cells seeded at a density of 5×10^4 cells per well in a 24-well plate were transfected with 5 nM siRNA using lipofectamine RNAiMAX (Qiagen) following the manufacturer's instructions.

Luciferase Assay. Gaussia luciferase activity was measured in supernatant from cells transfected with Gluc replicons derived from the HEV 83-2, p6, and Sar55 clones. Culture medium was collected daily and stored at 4 °C until measurement. Luciferase activity was measured after addition of 60 μL coelenterazine substrate (0.8 μM) to 10 μL of culture medium for 1 s using a GloMax® 20/20 Luminometer (Promega).

Drug Inhibition Assay. Cells electroporated with Gluc replicon constructs were treated with drugs at 10 μM, 30 μM, and 50 μM from days 3 to 5 post-electroporation with daily culture medium changes. Supernatant was collected on day 5 and subjected to luciferase assay as described above.

Cell Viability. Cells were incubated for 2 h at 37 °C with WST-1 (Sigma-Aldrich) diluted 1:100 in complete DMEM. One hundred μL of supernatant was transferred to the well of a 96-well plate and optical density was measured at 450 and 595 nm using the Multiskan Ascent Microplate Reader (Thermo Fisher Scientific).

Immunofluorescence and Western-Blot. Detailed procedures are described in *SI Appendix*.

Virus Infection. Huh-7.5 cells were seeded onto glass coverslip in a 24-well plate and infected 24 h later, in the presence of DMEM without FBS, with 10 μL of HEV p6 inoculum prepared as described in Supplementary Information. An inoculum inactivated by heat at 70 °C for 5 min was used as control. Twenty-four hours post-infection, culture medium was replaced by complete DMEM. Cells were fixed at day 5 post-infection for 10 min with paraformaldehyde 4% at 20 °C before immunofluorescence detection of ORF2 protein.

Fluorescence In Situ Hybridization. The RNAscope® Fluorescent Multiplex Reagent Kit (Advanced Cell Diagnostics) was used for fluorescence in situ hybridization (FISH). Cells were fixed with formaldehyde 10% for 30 min at 20 °C, washed twice with PBS and incubated with PBS-Triton X-100 0.1% for 10 min at 20 °C. Cells were then subjected to hybridization for 2.5 h at 40 °C with RNAscope probe V-HEV-p6-ORF1-O2-C2 to detect positive-strand RNA from the HEV p6 or 83-2 strain, or with probe V-HEV-p6-ORF2-sense-C3 to detect negative-strand RNA from the HEV p6 strain, diluted 1:50 in probe diluent. Cells were washed with washing buffer and incubated successively with amplification solutions Amp 1-FL (30 min at 40 °C), Amp 2-FL (15 min at 40 °C), Amp 3-FL (30 min at 40 °C), and Amp 4-FL (15 min at 40 °C in the dark), with two washes with washing buffer between each incubation. Following FISH, cells were blocked with PBS-BSA 3% for 15 min at 20 °C in the dark and subjected to immunofluorescence as described in *SI Appendix*.

Statistical Analyses. Significance values were calculated by applying one-way ANOVA followed by either Dunnett's or Tukey's multiple comparison test with the GraphPad Prism 9 software package (GraphPad Software).

Data, Materials, and Software Availability. All data are included in the manuscript and/or *SI Appendix*. Raw data, including MAGECK analysis, confocal images, luciferase assays, and WB analyses have been deposited in Zenodo (https://doi.org/10.5281/zenodo.7745883) (67).

ACKNOWLEDGMENTS. The authors gratefully acknowledge Jean Gruenberg and Konstantinos Petrovas for helpful discussion, Angela Pollán for expert technical assistance as well as Viet Loan Dao Thi, Suzanne U. Emerson, Koji Ishii, Volker Lohmann, Charles M. Rice, Didier Trono, Rainer G. Ulrich, Takaji Wakita, Feng Zhang and Qing Zhong for sharing reagents. Confocal laser scanning microscopy was performed at the BSL2 Biocontained Confocal Microscopy Facility of the Institute of Microbiology of Lausanne University Hospital and the University of Lausanne. Next-generation sequencing was performed at the Genomic Technologies Facility of the University of Lausanne. This work was supported by the Swiss National Science Foundation (grants 31003A_179424 and 31003A_207477 to D.M.) and the Novartis Foundation (18C140 to D.M.).

1. N. Kamar *et al.*, Hepatitis E virus infection. *Nat. Rev. Dis. Primers* **3**, 17086 (2017).
2. EASL, Easl clinical practice guidelines on hepatitis E virus infection. *J. Hepatol.* **68**, 1256–1271 (2018).
3. M. A. Purdy *et al.*, ICTV virus taxonomy profile: Hepeviridae 2022. *J. Gen. Virol.* **103**, 001778 (2022).
4. H. R. Dalton *et al.*, Hepatitis E virus and neurological injury. *Nat. Rev. Neurol.* **12**, 77–85 (2016).
5. Y. Debing, D. Moradpour, J. Neyts, J. Gouttenoire, Update on hepatitis E virology: Implications for clinical practice. *J. Hepatol.* **65**, 200–212 (2016).
6. I. Nimgaonkar, Q. Ding, R. E. Schwartz, A. Ploss, Hepatitis E virus: Advances and challenges. *Nat. Rev. Gastroenterol. Hepatol.* **15**, 96–110 (2018).
7. J. Gouttenoire *et al.*, Palmitoylation mediates membrane association of hepatitis E virus ORF3 protein and is required for infectious particle secretion. *PLoS Pathog.* **14**, e1007471 (2018).
8. C. J. Neufeldt, M. Cortese, Membrane architects: How positive-strand RNA viruses restructure the cell. *J. Gen. Virol.* **103**, 001773 (2022).
9. N. Oechslin, D. Moradpour, J. Gouttenoire, On the host side of the hepatitis E virus life cycle. *Cells* **9**, 1294 (2020).
10. M. H. Wissing, Y. Bruggemann, E. Steinmann, D. Todt, Virus–host cell interplay during hepatitis E virus infection. *Trends Microbiol.* **29**, 309–319 (2021).
11. H. Ma *et al.*, A CRISPR-based screen identifies genes essential for West-Nile-virus-induced cell death. *Cell Rep.* **12**, 673–683 (2015).
12. W. M. Schneider *et al.*, Genome-scale identification of SARS-CoV-2 and pan-coronavirus host factor networks. *Cell* **184**, 120–132.e114 (2021).
13. C. D. Marceau *et al.*, Genetic dissection of Flaviviridae host factors through genome-scale CRISPR screens. *Nature* **535**, 159–163 (2016).
14. H. Ma *et al.*, LDLRAD3 is a receptor for Venezuelan equine encephalitis virus. *Nature* **588**, 308–314 (2020).
15. N. E. Sanjana, O. Shalem, F. Zhang, Improved vectors and genome-wide libraries for CRISPR screening. *Nat. Methods* **11**, 783–784 (2014).
16. D. Szkolnicka *et al.*, Recombinant hepatitis E viruses harboring tags in the ORF1 protein. *J. Virol.* **93**, e00459-19 (2019).
17. G. Savidis *et al.*, Identification of Zika virus and dengue virus dependency factors using functional genomics. *Cell Rep.* **16**, 232–246 (2016).
18. B. Shue *et al.*, Genome-wide CRISPR screen identifies RACK1 as a critical host factor for flavivirus replication. *J. Virol.* **95**, e0059621 (2021).
19. W. Li *et al.*, MAGeCK enables robust identification of essential genes from genome-scale CRISPR/Cas9 knockout screens. *Genome Biol.* **15**, 554 (2014).
20. R. Farhat *et al.*, Identification of GBF1 as a cellular factor required for hepatitis E virus RNA replication. *Cell Microbiol.* **20**, e12804 (2018).
21. S. Hoffenberg *et al.*, A novel membrane-anchored Rab5 interacting protein required for homotypic endosome fusion. *J. Biol. Chem.* **275**, 24661–24669 (2000).
22. M. A. Fouraux *et al.*, 'Rabip4' is an effector of rab5 and rab4 and regulates transport through early endosomes. *Mol. Biol. Cell* **15**, 611–624 (2004).
23. C. M. Hunker *et al.*, Rab5-activating protein 6, a novel endosomal protein with a role in endocytosis. *Biochem. Biophys. Res. Commun.* **340**, 967–975 (2006).
24. C. S. Wegner *et al.*, Ultrastructural characterization of giant endosomes induced by GTPase-deficient Rab5. *Histochem. Cell Biol.* **133**, 41–55 (2010).
25. H. Stenmark *et al.*, Inhibition of rab5 GTPase activity stimulates membrane fusion in endocytosis. *EMBO J.* **13**, 1287–1296 (1994).
26. N. Oechslin *et al.*, Hepatitis E virus RNA-dependent RNA polymerase is involved in RNA replication and infectious particle production. *Hepatology* **75**, 170–181 (2022).
27. M. S. Pols, J. Klumperman, Trafficking and function of the tetraspanin CD63. *Exp. Cell Res.* **315**, 1584–1592 (2009).
28. J. Zhang *et al.*, Structure-based discovery of neoandrographolide as a novel inhibitor of Rab5 to suppress cancer growth. *Comput. Struct. Biotechnol. J.* **18**, 3936–3946 (2020).
29. A. McCluskey *et al.*, Building a better dynasore: The dyngo compounds potently inhibit dynamin and endocytosis. *Traffic* **14**, 1272–1289 (2013).
30. E. Macia *et al.*, Dynasore, a cell-permeable inhibitor of dynamin. *Dev. Cell* **10**, 839–850 (2006).
31. X. Cai *et al.*, PIKfyve, a class III PI kinase, is the target of the small molecular IL-12/IL-23 inhibitor apilimod and a player in Toll-like receptor signaling. *Chem. Biol.* **20**, 912–921 (2013).
32. T. Shiota *et al.*, The hepatitis E virus capsid C-terminal region is essential for the viral life cycle: Implication for viral genome encapsidation and particle stabilization. *J. Virol.* **87**, 6031–6036 (2013).
33. P. Shukla *et al.*, Adaptation of a genotype 3 hepatitis E virus to efficient growth in cell culture depends on an inserted human gene segment acquired by recombination. *J. Virol.* **86**, 5697–5707 (2012).
34. S. U. Emerson *et al.*, Recombinant hepatitis E virus genomes infectious for primates: Importance of capping and discovery of a cis-reactive element. *Proc. Natl. Acad. Sci. U.S.A.* **98**, 15270–15275 (2001).
35. R. Greco *et al.*, Improving the safety of cell therapy with the TK-suicide gene. *Front. Pharmacol.* **6**, 95 (2015).
36. F. Candotti *et al.*, Use of a herpes thymidine kinase/neomycin phosphotransferase chimeric gene for metabolic suicide gene transfer. *Cancer Gene. Ther.* **7**, 574–580 (2000).
37. K. Chockalingam, R. L. Simeon, C. M. Rice, Z. Chen, A cell protection screen reveals potent inhibitors of multiple stages of the hepatitis C virus life cycle. *Proc. Natl. Acad. Sci. U.S.A.* **107**, 3764–3769 (2010).
38. Q. Ren *et al.*, A Dual-reporter system for real-time monitoring and high-throughput CRISPR/Cas9 library screening of the hepatitis C virus. *Sci. Rep.* **5**, 8865 (2015).
39. M. Stone, S. Jia, W. D. Heo, T. Meyer, K. V. Konan, Participation of rab5, an early endosome protein, in hepatitis C virus RNA replication machinery. *J. Virol.* **81**, 4551–4563 (2007).
40. C. New *et al.*, Tetraspanins: Host factors in viral infections. *Int. J. Mol. Sci.* **22**, 11609 (2021).
41. M. Matsuda *et al.*, Alternative endocytosis pathway for productive entry of hepatitis C virus. *J. Gen. Virol.* **95**, 2658–2667 (2014).
42. J. L. Martinez, C. F. Arias, Role of the guanine nucleotide exchange factor GBF1 in the replication of RNA viruses. *Viruses* **12**, 682 (2020).
43. I. Nimgaonkar *et al.*, Isocotoin suppresses hepatitis E virus replication through inhibition of heat shock protein 90. *Antiviral. Res.* **185**, 104997 (2021).
44. F. Zhang *et al.*, Targeting proteostasis of the HEV replicase to combat infection in preclinical models. *J. Hepatol.* **78**, 704–716 (2023).
45. M. Surjit, R. Oberoi, R. Kumar, S. K. Lal, Enhanced alpha1 microglobulin secretion from Hepatitis E virus ORF3-expressing human hepatoma cells is mediated by the tumor susceptibility gene 101. *J. Biol. Chem.* **281**, 8135–8142 (2006).
46. S. Nagashima *et al.*, A PSAP motif in the ORF3 protein of hepatitis E virus is necessary for virion release from infected cells. *J. Gen. Virol.* **92**, 269–278 (2011).
47. S. Nagashima *et al.*, Tumour susceptibility gene 101 and the vacuolar protein sorting pathway are required for the release of hepatitis E virions. *J. Gen. Virol.* **92**, 2838–2848 (2011).
48. S. Nagashima *et al.*, Hepatitis E virus egress depends on the exosomal pathway, with secretory exosomes derived from multivesicular bodies. *J. Gen. Virol.* **95**, 2166–2175 (2014).
49. J. Perttila, P. Spuul, T. Ahola, Early secretory pathway localization and lack of processing for hepatitis E virus replication protein pORF1. *J. Gen. Virol.* **94**, 807–816 (2013).
50. S. Rehman, N. Kapur, H. Durgapal, S. K. Panda, Subcellular localization of hepatitis E virus (HEV) replicase. *Virology* **370**, 77–92 (2008).
51. K. Metzger *et al.*, Processing and subcellular localization of the hepatitis E virus replicase: Identification of candidate viral factories. *Front. Microbiol.* **13**, 828636 (2022).
52. S. Nagashima *et al.*, Characterization of the quasi-enveloped hepatitis E virus particles released by the cellular exosomal pathway. *J. Virol.* **91**, e00822-17 (2017).
53. A. Nazli *et al.*, LAMP3/CD63 expression in early and late endosomes in human vaginal epithelial cells is associated with enhancement of HSV-2 infection. *J. Virol.* **96**, e0155322 (2022).
54. L. Grassel *et al.*, The CD63–Syntenin-1 complex controls post-endocytic trafficking of oncogenic human papillomaviruses. *Sci. Rep.* **6**, 32337 (2016).
55. S. N. Hurwitz, M. R. Cheerathodi, D. Nkosi, S. B. York, D. G. Meckes Jr., Tetraspanin CD63 bridges autophagic and endosomal processes to regulate exosomal secretion and intracellular signaling of Epstein–Barr virus LMP1. *J. Virol.* **92**, e01969-17 (2018).
56. S. Miller, J. Krijnse-Locker, Modification of intracellular membrane structures for virus replication. *Nat. Rev. Microbiol.* **6**, 363–374 (2008).
57. D. J. Barton, S. G. Sawicki, D. L. Sawicki, Solubilization and immunoprecipitation of alphavirus replication complexes. *J. Virol.* **65**, 1496–1506 (1991).
58. P. Kujala *et al.*, Biogenesis of the Semliki Forest virus RNA replication complex. *J. Virol.* **75**, 3873–3884 (2001).
59. S. Froshauer, J. Kartenbeck, A. Helenius, Alphavirus RNA replicase is located on the cytoplasmic surface of endosomes and lysosomes. *J. Cell Biol.* **107**, 2075–2086 (1988).
60. X. Yin, C. Ambardekar, Y. Lu, Z. Feng, Distinct entry mechanisms for nonenveloped and quasi-enveloped hepatitis E viruses. *J. Virol.* **90**, 4232–4242 (2016).
61. K. J. Blight, J. A. McKeating, C. M. Rice, Highly permissive cell lines for subgenomic and genomic hepatitis C virus RNA replication. *J. Virol.* **76**, 13001–13014 (2002).
62. T. T. Chen *et al.*, Establishment and characterization of a cancer cell line derived from an aggressive childhood liver tumor. *Pediatr. Blood Cancer* **53**, 1040–1047 (2009).
63. H. T. Nguyen, P. Shukla, U. Torian, K. Faulk, S. U. Emerson, Hepatitis E virus genotype 1 infection of swine kidney cells in vitro is inhibited at multiple levels. *J. Virol.* **88**, 868–877 (2014).
64. A. L. Szymczak, D. A. Vignali, Development of 2A peptide-based strategies in the design of multicistronic vectors. *Expert. Opin. Biol. Ther.* **5**, 627–638 (2005).
65. Q. Sun, W. Westphal, K. N. Wong, I. Tan, Q. Zhong, Rubicon controls endosome maturation as a Rab7 effector. *Proc. Natl. Acad. Sci. U.S.A.* **107**, 19338–19343 (2010).
66. C. Zhang *et al.*, An RNA interference/Adeno-associated virus vector-based combinatorial gene therapy approach against hepatitis E virus. *Hepatol. Commun.* **6**, 878–888 (2022).
67. N. Oechslin, N. Da Silva, M. Ankavay, D. Moradpour, J. Gouttenoire, A Genome-Wide CRISPR/Cas9 Screen Identifies a Role for Rab5A and Early Endosomes in Hepatitis E Virus Replication. Dataset. https://doi.org/10.5281/zenodo.7745883. Deposited 17 March 2023.